Rapid Non-Linear Uncertainty Propagation via Analytical Techniques

Kohei Fujimoto and Daniel J. Scheeres
University of Colorado-Boulder, United States

ABSTRACT

Situational awareness of Earth-orbiting particles is known to be both a data starved and well-modeled problem. These two ideas are combined in this paper: a method of analytically propagating non-linear orbit uncertainties is discussed. In particular, the uncertainty is expressed as an analytic probability density function for all time, which is powerful as propagation is only a matter of changing the time parameter. Even when closed-form expressions are not available for a given system, solutions in tractable series form exist. Due to the large uncertainties and potentially long mapping time-spans, even initially Gaussian PDFs may become significantly non-Gaussian.

1. INTRODUCTION

Situational awareness of Earth-orbiting particles such as active satellites and space debris is known to be a *data starved* problem compared to traditional orbit estimation problems in that objects may not be observed for days if not weeks [7]. Therefore, consistent characterization of the uncertainty associated with these objects is crucial in maintaining an accurate catalog of objects in Earth orbit. As such, recently in astrodynamics, much attention has been given to the non-linear deformation of uncertainty for the orbiter problem [3, 5, 6, 8]. Simultaneously, the motion of satellites in Earth orbit is *well-modeled* in that it is particularly amenable to having their solution and their uncertainty described through analytic or semi-analytic techniques [2, 17]. Even when stronger non-gravitational perturbations such as solar radiation pressure and atmospheric drag are encountered, these perturbations generally have deterministic components that are substantially larger than their time-varying stochastic components [9, 11].

These two ideas are combined in this paper: a method of analytically propagating non-linear orbit uncertainties is discussed. In particular, the uncertainty is expressed as an analytic probability density function (pdf) for all time. For a deterministic system model, such pdfs may be obtained if the initial pdf and the system states for all time are also given analytically. Even when closed-form solutions are not available, approximate solutions exist in the form of Edgeworth series for pdfs and Taylor series for the states. The coefficients of the latter expansion are referred to as state transition tensors (STTs), which are a generalization of state transition matrices to arbitrary order. Due to the large uncertainties and potentially long mapping time-spans, even initially Gaussian pdfs become significantly non-Gaussian.

Analytically expressed pdfs can be incorporated in many practical tasks in space situational awareness (SSA). One can compute the mean and covariance of the uncertainty, for example, with the moments of the initial pdf as inputs. This process does not involve any sampling and under two-body dynamics, its accuracy can be determined a priori [5]. Analytical pdfs may also be incorporated in a non-linear Bayesian estimator for orbit determination and conjunction assessment [16]. Finally, model parameter uncertainty, such as those for atmospheric drag, is readily implemented with little additional computational burden by adding the parameters in the state vector.

The outline of this paper is as follows. Necessary mathematical concepts are first introduced (*Background*), such as the Fokker-Plank equation, STTs, and King-Hele's analytical theory of orbital motion in an atmosphere (*Background*). This theoretical framework is implemented numerically in MATLAB (*Results*). For a circular orbit, the 3-σ error ellipsoid, mean, and covariance of a Gaussian distribution in both state and parameter space is propagated using the STT approach. These results are compared with those obtained from Monte Carlo simulations using the NRLMSISE-00 density model [13]. We find that the STT is an efficient method of uncertainty propagation even when non-conservative forces exist in the dynamics.

2. BACKGROUND

In this section, the solution of the Fokker-Planck equation for a deterministic dynamical system including non-conservative forces as well as the state transition tensor concept are formally introduced.

2.1. Solution of the Fokker-Planck Equation For a Deterministic Dynamical System

Suppose the dynamics of some system is expressed as

$$\dot{\mathbf{X}} = \boldsymbol{f}(t, \mathbf{X}), \tag{1}$$

where $\mathbf{X}$ is the state vector and $\boldsymbol{f}$ are the equations of motion [5, 12]. Then, the solution of (1) is expressed as

$$\mathbf{X}(t) = \boldsymbol{\phi}(t; \mathbf{X}^0, t^0), \tag{2}$$

where superscript 0 indicates initial conditions. $\boldsymbol{\phi}$ must satisfy the following conditions

$$\frac{\mathrm{d}\boldsymbol{\phi}}{\mathrm{d}t} = \boldsymbol{f}(t, \boldsymbol{\phi}(t; \mathbf{X}^0, t)) \tag{3}$$

$$\boldsymbol{\phi}(t^0; \mathbf{X}^0, t^0) = \mathbf{X}^0. \tag{4}$$

One can define the inverse solution flow $\boldsymbol{\psi}(t, \mathbf{X}; t^0)$

$$\mathbf{X}^0 = \boldsymbol{\psi}(t, \mathbf{X}; t^0) \tag{5}$$

which maps a current state back to the initial epoch. For a general solution flow, the inverse flow can be found by interchanging the initial and final states

$$\boldsymbol{\psi}(t, \mathbf{X}; t^0) = \boldsymbol{\phi}(t^0; \mathbf{X}, t). \tag{6}$$

For a system that satisfies the Itô stochastic differential equation, the time evolution of a probability density function (pdf) $p(\mathbf{X}, t)$ over $\mathbf{X}$ at time t is described by the Fokker-Planck equation [10]

$$\frac{\partial p(\mathbf{X}, t)}{\partial t} = -\sum_{i=1}^{n} \frac{\partial}{\partial \mathbf{X}_i} \left\{ p(\mathbf{X}, t) \boldsymbol{f}_i(\mathbf{X}, t) \right\} + \frac{1}{2} \sum_{i=1}^{n} \sum_{j=1}^{n} \frac{\partial^2}{\partial \mathbf{X}_i \partial \mathbf{X}_j} \left[p(\mathbf{X}, t) \left\{ G(\mathbf{X}, t) Q(t) G^{\mathrm{T}}(\mathbf{X}, t) \right\}_{ij} \right], \tag{7}$$

where a single subscript indicates vector components and a double subscript indicates matrix components. Matrices G and Q characterize the diffusion. For a deterministic dynamical system, whether or not it is Hamiltonian, it can be shown that the probability $\Pr(\mathbf{X} \in \mathcal{B})$ over some volume $\mathcal{B}$ in phase space is an integral invariant [12, 14, 15]

$$\Pr(\mathbf{X} \in \mathcal{B}) = \int_{\mathcal{B}} p[\mathbf{X}(t)] \mathrm{d}\mathbf{X} = \int_{\mathcal{B}^0} p[\boldsymbol{\phi}(t; \mathbf{X}^0, t^0)] \left| \frac{\partial \mathbf{X}}{\partial \mathbf{X}^0} \right| \mathrm{d}\mathbf{X}^0 = \int_{\mathcal{B}^0} p(\mathbf{X}^0) \mathrm{d}\mathbf{X}^0, \tag{8}$$

where $p[\mathbf{X}(t)]$ is the probability density function (pdf), $\mathcal{B}^0$ is the volume that corresponds to $\mathcal{B}$ at the initial time, and $|\cdot|$ is the determinant operator. Consequently, [1]

$$p[\boldsymbol{\phi}(t; \mathbf{X}^0, t^0)] = p(\mathbf{X}^0) \left| \frac{\partial \mathbf{X}}{\partial \mathbf{X}^0} \right|^{-1}. \tag{9}$$

The inverse of the determinant makes up for the change in phase volume due to the non-conservative forces in the system. For a Hamiltonian system, $|\partial \mathbf{X} / \partial \mathbf{X}^0| = 1$ from Liouville's Theorem (i.e. phase volume is conserved), so we find

$$p[\boldsymbol{\phi}(t; \mathbf{X}^0, t^0)] = p(\mathbf{X}^0). \tag{10}$$

Note that for any deterministic system, as long as both the solution flow of the dynamics and the initial pdf are know analytically, the pdf for all time can also be expressed analytically. If one cannot obtain an analytical solution flow, it nevertheless may be approximated by a Taylor series expansion via state transition tensors: details on this method are explained in subsequent sections. Analytical expressions of the pdf are useful because propagation is then only a matter of changing the time parameter t.

2.2. Non-Linear Mapping of System Dynamics using State Transition Tensors

One method of obtaining an analytical, non-linear approximation to solution flow $\boldsymbol{\phi}(t; \mathbf{X}^0, t^0)$ is to use a concept called the *state transition tensor* (STT). If a Taylor series expansion of the solution function (2) is taken about some reference trajectory $\mathbf{X}^*$, the state deviation $\mathbf{x} = \mathbf{X} - \mathbf{X}^*$ is

$$\mathbf{x}_i(t) = \sum_{p=1}^{m} \frac{1}{p!} \Phi_{i,k_1 \dots k_p} \mathbf{x}^0_{k_1} \dots \mathbf{x}^0_{k_p}, \tag{11}$$

where the subscripts indicate the component of each tensor, m is the order of the expansion and Φ is defined to be the STT of order p [12]. Einstein's summation notation is used, and the comma in the subscript simply denotes that the i-th component is not summed over. Note that the STT is a generalization of the state transition matrix to any arbitrary order. For $m = 1$, the result is familiar:

$$\mathbf{x}_i(t) = \Phi_{i,k_1} \mathbf{x}^0_{k_1} \Rightarrow \mathbf{x}(t) = [\Phi]\mathbf{x}^0. \tag{12}$$

Given the solution flow $\boldsymbol{\phi}$, the STT can be explicitly solved for:

$$\Phi_{i,k_1 \dots k_p} = \left. \frac{\partial^p \mathbf{X}_i}{\partial \mathbf{X}^0_{k_1} \dots \partial \mathbf{X}^0_{k_p}} \right|_*, \tag{13}$$

where the subscript $*$ indicates that Φ is evaluated over the reference trajectory $\mathbf{X}^*$. If $\mathbf{X}$ is not given as a function of $\mathbf{X}^0$, then the following differential equation can be solved

$$\dot{\Phi}_{i,k_1 \dots k_p} = G(A_{i,k_1}, \dots, A_{i,k_1 \dots k_p}; \Phi_{i,k_1}, \dots, \Phi_{i,k_1 \dots k_p}), \tag{14}$$

where

$$A_{i,k_1 \dots k_p} = \left. \frac{\partial^p \boldsymbol{f}_i}{\partial \mathbf{X}_{k_1} \dots \mathbf{X}_{k_p}} \right|_* \tag{15}$$

is the local dynamics tensor, and G is a function described in Fujimoto, et al [5]. Note that A and G are the generalization of the linear dynamics matrix to any arbitrary order. Again, when $m = 1$, the result is familiar:

$$\dot{\Phi}_{i,k_1} = A_{i,l_1} \Phi_{l_1,k_1} \Rightarrow [\dot{\Phi}] = [A][\Phi]. \tag{16}$$

2.3. Non-Linear Mapping of Probability Cumulants using State Transition Tensors

Combining results from the above two sections, the mean $\mathbf{M}(t) = \mathbf{m}(t) + \mathbf{X}^*(t)$ of a pdf $p[\mathbf{X}(t)]$ can be propagated non-linearly as

$$\mathbf{M}(t) = \int_\infty \mathbf{X}(t) p[\mathbf{X}(t)] \mathrm{d}\mathbf{X} = \int_\infty \boldsymbol{\phi}(t; \mathbf{X}^0, t^0) p(\mathbf{X}^0) \left| \frac{\partial \mathbf{X}}{\partial \mathbf{X}^0} \right|^{-1} \mathrm{d}\mathbf{X}^0 \tag{17}$$

$$\Leftrightarrow \mathbf{m}_i(t) = \sum_{p=1}^{m} \frac{1}{p!} \Phi_{i,k_1 \dots k_p} \int_\infty p(\mathbf{x}^0) \left| \frac{\partial \mathbf{X}}{\partial \mathbf{X}^0} \right|^{-1} \mathbf{x}^0_{k_1} \dots \mathbf{x}^0_{k_p} \mathrm{d}\mathbf{x}^0. \tag{18}$$

Similarly, the covariance matrix $[P](t)$ is propagated as

$$[P](t) = \int_\infty [\mathbf{X}(t) - \mathbf{M}(t)]^{\mathrm{T}} [\mathbf{X}(t) - \mathbf{M}(t)] p[\mathbf{X}(t)] \mathrm{d}\mathbf{X} \tag{19}$$

$$= \int_\infty [\boldsymbol{\phi}(t; \mathbf{X}^0, t^0) - \mathbf{M}(t)]^{\mathrm{T}} [\boldsymbol{\phi}(t; \mathbf{X}^0, t^0) - \mathbf{M}(t)] p(\mathbf{X}^0) \left| \frac{\partial \mathbf{X}}{\partial \mathbf{X}^0} \right|^{-1} \mathrm{d}\mathbf{X}^0 \tag{20}$$

$$\Leftrightarrow [P]_{ij}(t) = \left[\sum_{p=1}^{m} \sum_{q=1}^{m} \frac{1}{p!q!} \Phi_{i,k_1 \dots k_p} \Phi_{j,l_1 \dots l_q} \int_\infty p(\mathbf{x}^0) \left| \frac{\partial \mathbf{X}}{\partial \mathbf{X}^0} \right|^{-1} \mathbf{x}^0_{k_1} \dots \mathbf{x}^0_{k_p} \mathbf{x}^0_{l_1} \dots \mathbf{x}^0_{l_q} \mathrm{d}\mathbf{x}^0 \right] - \mathbf{m}_i(t) \mathbf{m}_j(t) \tag{21}$$

Again, for Hamiltonian systems, $|\partial \mathbf{X}/\partial \mathbf{X}^0| = 1$, so the results simplifies to

$$\mathbf{m}_i(t) = \sum_{p=1}^{m} \frac{1}{p!} \Phi_{i,k_1 \ldots k_p} E\left[\mathbf{x}_{k_1}^0 \ldots \mathbf{x}_{k_p}^0\right] \tag{22}$$

$$[P]_{ij}(t) = \left(\sum_{p=1}^{m} \sum_{q=1}^{m} \frac{1}{p!q!} \Phi_{i,k_1 \ldots k_p} \Phi_{j,l_1 \ldots l_q} E\left[\mathbf{x}_{k_1}^0 \ldots \mathbf{x}_{k_p}^0 \mathbf{x}_{l_1}^0 \ldots \mathbf{x}_{l_q}^0\right] \right) - \mathbf{m}_i(t)\mathbf{m}_j(t), \tag{23}$$

where E is the expected value operator

$$E[f(\mathbf{x})] = \int_{\infty} f(\mathbf{x}) p[\mathbf{x}(t)] \mathrm{d}\mathbf{x}. \tag{24}$$

2.4. Analytic Dynamics For a Circular Orbit With Atmospheric Drag

Here, we introduce the analytical motion of an object in a circular orbit subject to atmospheric drag as derived by King-Hele [9]. We then derive the STTs. Similar results are available for elliptic orbits [4]. Some important assumptions are:

- The atmosphere is spherically symmetrical
- The atmospheric density model is exponential with constant parameters in time
- The atmosphere rotates at the same angular rate as the Earth
- The Earth's gravitational field is approximated as a point mass

If a more detailed dynamical model is desired, the STTs may still be computed semi-analytically via (14). Note that secular effects due to the J_2 oblateness term in the gravitational potential may be readily included [5]. The following initial states and dynamical system parameters are used in this section unless otherwise noted

$$a^0 = 6678.1 \text{ km}, i^0 = 0.26179 \text{ rad}, \omega_E = 7.2722 \times 10^{-5} \text{ rad/s}, \mu = 398600 \,\mathrm{km}^3\mathrm{s}^{-2}, \tag{25}$$

where a is semi-major axis, i is the inclination, ω_E is the Earth's rotational rate, and μ is the standard gravitational parameter. The initial orbit period is thus 90.52 minutes. The atmospheric parameters are

$$H = 40 \text{ km}, \rho^* = 10^{-2} \,\mathrm{kg/km}^3, \mathrm{BC} = 10^2 \,\mathrm{kg/m}^2, \tag{26}$$

where H is scale height, ρ is atmospheric density, BC is the ballistic coefficient, and superscript * indicates that the value is at the reference altitude of 300 km; i.e. $a^* = 6678.1$ km.

For an initial circular orbit, only the semi-major axis, and consequently the mean anomaly, change with time due to drag effects. The semi-major axis is given as a function of time as

$$a(t; a^0) = a^0 + H \ln\left[1 - \frac{2\pi\delta\rho^*(a^0)^2 \mathrm{e}^{\beta(a^* - a^0)} t}{HT^0}\right] = a^0 + H\ln(1 + \epsilon t), \tag{27}$$

where

$$T^0 = 2\pi\sqrt{\frac{(a^0)^3}{\mu}} \tag{28}$$

$$\delta = \frac{(1 - a^0\omega_E\sqrt{a^0/\mu}\cos i^0)^2}{\mathrm{BC}} \tag{29}$$

$$\epsilon = -\frac{2\pi\delta\rho^*(a^0)^2 \mathrm{e}^{\beta(a^* - a^0)}}{HT^0}, \tag{30}$$

Next, to find the mean anomaly, the mean motion $n(t)$ is integrated over time

$$M(t; a^0, M^0) = M^0 + \int_0^t n(t)\mathrm{d}\tau = M^0 + \int_0^t \sqrt{\frac{\mu}{a(\tau)^3}}\mathrm{d}\tau. \tag{31}$$

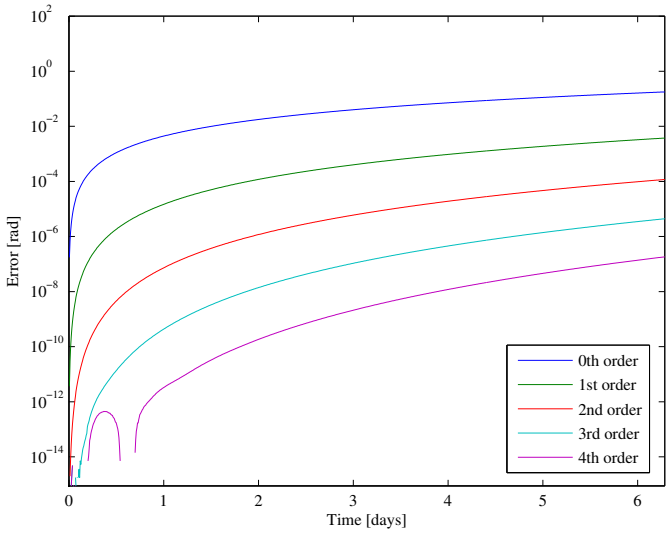

Figure 1: The difference in the numerically and analytically integrated mean anomaly (i.e. "Error") for different orders of expansion of mean motion n. The reference orbit is a 300 km altitude circular orbit with an inclination of $15°$. The errors are plotted for up to 100 orbit periods of the initial orbit.

Now, for $a \sim 6700$ km and greater, ϵ is often very small ($\sim 10^{-8}$). Therefore, n may be expanded as a polynomial of ϵ:

$$\frac{n(t)}{\sqrt{\mu}} = \frac{1}{(a^0)^{3/2}} - \frac{3H\epsilon t}{2(a^0)^{5/2}} + \mathcal{O}(\epsilon^2), \tag{32}$$

which allows for the analytical integration of (31)

$$M \approx M^0 + \sqrt{\frac{\mu}{(a^0)^3}}t - \frac{3H\epsilon}{4}\sqrt{\frac{\mu}{(a^0)^5}}t^2. \tag{33}$$

Note that for a 300 km altitude circular orbit, a fourth-order expansion of n with respect to ϵ results in $\sim 10^{-7}$ radian accuracy in mean anomaly ($\sim 10^0$ meter accuracy in in-track position) after 100 periods of the initial orbit; refer to Figure 1 for details. The object drops about 2.5 km in altitude over this time.

Regarding the STTs, the only non-zero values are

$$\frac{\partial M}{\partial M^0}, \frac{\partial^i a}{\partial (a^0)^i}, \frac{\partial^i M}{\partial (a^0)^i}, \tag{34}$$

where i goes up to the order of the expansion. Since $a(t; a^0)$ and $M(t; a^0, M^0)$ are known explicitly, the STTs can also be solved for via (13). Now, for this system, we note that $|\partial \mathbf{X}/\partial \mathbf{X}^0| = \partial a/\partial a^0$, which simplifies to the form

$$\frac{\partial a}{\partial a^0} = 1 + \frac{N_1/N_2 - 1}{N_3/N_2\, t^{-1} + 1}, \tag{35}$$

where

$$N_1 = \frac{Ha^0}{2}\rho^* \mathrm{e}^{(a^* - a^0)/H}\left[-\sqrt{\frac{\mu}{a^0}}\mu + 8a^0\mu\omega_\mathrm{E}\cos i^0 - 7(a^0)^3\sqrt{\frac{\mu}{a^0}}\omega_\mathrm{E}^2\cos^2 i^0\right] \tag{36}$$

$$N_2 = -(a^0)^2\rho^* \mathrm{e}^{(a^* - a^0)/H}\left[\sqrt{\frac{\mu}{a^0}}\mu - 2a^0\mu\omega_\mathrm{E}\cos i^0 + (a^0)^3\sqrt{\frac{\mu}{a^0}}\omega_\mathrm{E}^2\cos^2 i^0\right] \tag{37}$$

$$N_3 = a^0 H \mathrm{BC}\mu \tag{38}$$

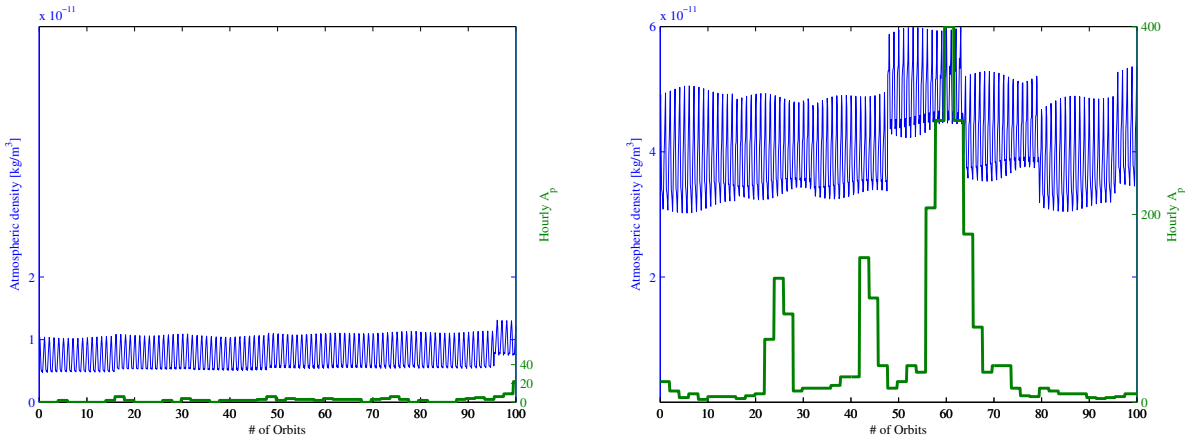

Figure 2: Atmospheric density at the reference state and the hourly A_p index startng February 8, 2009 (left, *Calm*) and July 11, 2000 (right, *Storm*). Units of time in orbit periods of the initial orbit (≈ 90.52 minutes).

But if we substitute values in (25), we find

$$\frac{N_1}{N_2} = 0.0018333, \frac{N_3}{N_2} = -8.7877 \times 10^6, \tag{39}$$

and so $\partial a / \partial a^0 = 1 + \varepsilon$ for practical values of propagation time t, where the absolute value $\|\varepsilon\| \ll 1$. In other words, the change in phase volume is negligible. When the cumulants are to be computed analytically, the problem may be simplified as being Hamiltonian without large errors: refer to Section 3.2 for details.

If we would like to consider uncertainty in parameter space, such as the ballistic coefficient, we add the parameters to the state variables. Again, assuming that atmospheric parameters are constant in time, the dynamics are simply

$$\frac{\mathrm{d}\,\mathrm{BC}}{\mathrm{d}t} = 0. \tag{40}$$

The partial derivatives (i.e. STTs) of the states with respect to the ballistic coefficient may still be solved explicitly.

3. RESULTS

In this section, results of a MATLAB implementation of the analytical theory discussed above is shown. A graphical representation is first given through the propagation of the 3-σ error ellipse. The propagation of cumulants of the pdf is then explored. Each result is compared to a numerically propagated Monte Carlo (MC) simulation.

3.1. Propagation of the 3-σ Ellipse

Demonstrated in this section is the analytical propagation of a 3-σ ellipse of an initial Gaussian distribution in the semi-major axis (a) / mean anomaly (M) / ballistic coefficient (BC) space. We consider the same circular orbit as in (25) with $\mathrm{BC} = 10^2\ \mathrm{kg/m^2}$ as the nominal orbit. Two simulation epoch are tested: February 8, 2009, which will be referred to as *Calm*, and July 11, 2000, referred to as *Storm* to indicate the intensity of geomagnetic activity. In each case, the uncertainty is propagated for 6.286 days. The central body is approximated as a point mass. Figure 2 shows the density and A_p geomagnetic index history for both epochs. Figure 3 is a representation of the initial distribution in the orbit elements. The data points are generated as follows:

MC Simulation 2,000 sample points are first distributed normally in the a-M space with a covariance

$$[P] = \begin{bmatrix} \sigma_a^2 & \mu_{aM} \\ & \sigma_M^2 \end{bmatrix} = \begin{bmatrix} (20\ \mathrm{km})^2 & 0 \\ & (0.01^\circ)^2 \end{bmatrix}. \tag{41}$$

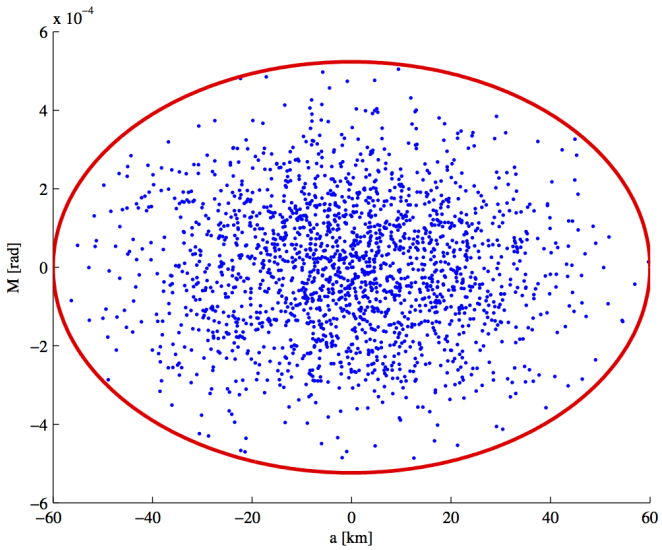

Figure 3: Initial Gaussian distribution in the a-M plane (sampled with the blue points) with the corresponding 3-σ ellipse (red curve).

The BC is allowed to fluctuate over time as a sinusoid

$$\mathrm{BC}(t) = \mathrm{BC}^0 + A_{\mathrm{BC}} \sin(\frac{2\pi}{\tau_{\mathrm{BC}}} t + \phi_{\mathrm{BC}}), \tag{42}$$

and the parameters $A_{\mathrm{BC}} \in [-2\times10, 2\times10]\,\mathrm{kg/m^2}$, $\tau_{\mathrm{BC}} \in [100, 10000]$ sec, $\phi_{\mathrm{BC}} \in [0, 2\pi]$ are picked randomly for each sample point. The drag accelerations are given as

$$\ddot{\mathbf{r}}_{\mathrm{drag}} = \frac{1}{2\mathrm{BC}} \rho V \mathbf{V}, \tag{43}$$

where $\mathbf{V}$ is the relative velocity of the spacecraft relative to the atmosphere. We assume that the atmosphere is spherical and rotates at the same rate as the Earth's daily rotation about its axis. The density ρ is simulated with the NRLMSISE-00 model [13].

STT Propagation 10^3 points are taken on the initial 3-σ ellipsoid where the uncertainty in the orbit elements is the same as the MC simulation and $\sigma_{\mathrm{BC}} = 5\,\mathrm{kg/m^2}$. Expansion of King-Hele's theory up to 4th order is considered. The reference density ρ^* and scale height H are determined by fitting the NRLMSISE-00 computed densities between altitudes of 240 km and 360 km over the first orbital period. We find $(\rho^*, H) = (7.262 \cdot 10^{-12}\,\mathrm{kg/km^3}, 36.49\,\mathrm{km})$ for the *Calm* scenario and $(3.897 \cdot 10^{-11}\,\mathrm{kg/km^3}, 55.22\,\mathrm{km})$ for *Storm*. For simplicity, n is expanded only up to first order in ϵ.

Figure 4 shows the results of the propagation. As expected, since probability is an integral invariant regardless of whether the system is conservative, the 3-σ curve converges upon the distribution of MC points as the order of the STT is increased. Indeed, due to the highly non-linear nature of the dynamics, many MC points fall outside of the linearly propagated uncertainty ellipsoid. Furthermore, by explicitly accounting for the uncertainty in BC, the analytic model succeeds in capturing the effects of time-varying ρ and BC. This result suggests that even though the drag force is stochastic, it has a dominant deterministic component whose uncertainties are sufficiently expressed as parametric errors. Therefore, computationally efficient analytic techniques are attractive option for uncertainty propagation.

3.2. Propagation of the Cumulants

In this section, we discuss a MATLAB implementation of the theory introduced in Section 2.3. Here, the initial uncertainty is assumed to be Gaussian as in (41) but only in the semi-major axis (a) and mean anomaly (M) directions;

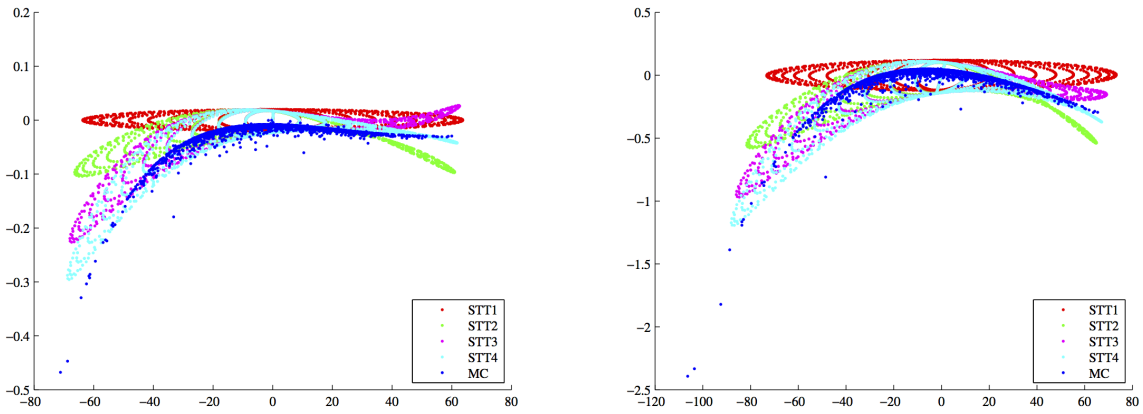

Figure 4: An initial Gaussian distribution propagated numerically (MC) and analytically (STT; number indicates expansion order) over 6.286 days for the *Calm* (left) and *Storm* (right) scenarios. The results are projected on the semi-major axis (a) / mean anomaly (M) space in units of km-rad and subsequently rotated so that the axes of the plot corresponds to the principal axis directions of the linearly propagated ellipse.

the ballistic coefficient is assumed to be constant at $\mathrm{BC} = 10^2\,\mathrm{kg/m^2}$. The central body is again approximated as a point mass. The mean and covariance are computed using both a numerical MC simulation and the analytical dynamics via the STT method:

MC simulation The initial distribution is sampled at 10^4 sample points that span across $\pm 6\sigma$ in both a and M. The moments of the pdf along with the Jacobian determinant are numerically integrated with (16), (17), and (20). We consider these results as the truth.

STT propagation Since the contraction of the state space is slow for objects with realistic parameters such as in (25), we assume $|\partial \mathbf{X}/\partial \mathbf{X}_0| \approx 1$ and thus compute the mean and covariance with (22) and (23), respectively. The dynamics are expanded up to 4th order, with the mean motion n expanded up to 1st order. All computation is analytic.

The same two epochs were tested (*Calm* and *Stormy*) and the uncertainty is propagated for 1.257 days; a shorter propagation time is chosen only to ensure that the Monte Carlo converges in a reasonable time. Table 1 shows the relative error of the STT propagated cumulants with respect to the MC simulation. Overall, the analytically propagated cumulants are within 1% relative error for all coordinate directions. The accuracy of the analytical covariance is consistently worse than the mean by an order of magnitude. A possible explanation is that the covariance can be thought of as a direct measure of the "volume" of the uncertainty, and thus is more strongly influenced by the phase volume contraction than the mean. Nevertheless, we may conclude that approximating the phase volume as constant when computing for pdf cumulants analytically is acceptable for many low area-to-mass ratio objects in LEO.

Table 1: Relative error of analytically propagated cumulants compared to a numerically computed truth.

	Rel. Err. Mean [%]		**Rel. Err. Cov. [%]**		
Scenario	$\bar{a}$	$\bar{M}$	σ_a^2	μ_{aM}	σ_M^2
Calm	0.0127	-0.0145	-0.5417	-0.1815	-0.3042
Stormy	0.0004	-0.0220	-0.7657	-0.5939	-0.4225

Finally, Table 2 compares computation time of cumulants between the Monte Carlo and STT methods on a Mac Pro workstation for the above example. Again, since the STTs are purely analytic, once the STTs have been solved for, all that is required for propagation is to change the time parameter accordingly. As a result, the STT propagation is not only many orders of magnitude faster than the Monte Carlo but also does not scale with propagation time

nor sampling resolution of the state space. Overall, the STT method is both accurate and efficient in non-linearly propagating uncertainty even in the presence of non-conservative forces.

Table 2: Computation time required to compute the mean and covariance with the Monte Carlo (MC) and STT techniques. The process is split up into uncertainty propagation (Prop.), and mean (Mean) and covariance computation (Cov.) The results are an average over the two simulation epochs considered.

	MC	**STT**
Prop. [s]	2.643×10^4	4.635×10^{-2}
Mean [s]	2.802×10^0	2.310×10^{-4}
Cov. [s]	2.429×10^0	3.580×10^{-4}
Total [s]	2.644×10^4	4.694×10^{-2}

4. CONCLUSIONS

In this paper, an analytical method of non-linear uncertainty propagation including non-conservative effects was discussed. A special solution to the Fokker-Planck equations for deterministic systems and the state transition tensor concept are combined so that, given an analytical expression of both the initial probability distribution and the dynamics, the probability distribution may be expressed analytically for all time. Propagation of uncertainty is then only a matter of changing the time parameter t. In particular, King-Hele's theory on orbital motion influenced by atmospheric drag was applied to the above framework and its propagation results were compared with a numerical Monte Carlo simulation with a realistic density model. This example demonstrated the potential efficiency and accuracy of analytical uncertainty propagation. Future work is to further incorporate additional perturbations relevant to Earth-orbiting objects, such as effects due to the oblateness of the Earth.

ACKNOWLEDGEMENTS

This research was supported by grants from the FAA Center of Excellence for Commercial Space Transportation, from the Air Force Office of Scientific Research Grant FA9550-11-1-0188, and by Numerica Corporation through an Air Force STTR grant. The authors would also like to thank Jason Leonard for his advice on incorporating the NRLMSISE-00 model in our simulations.

References

[1] J. L. Crassidis and J. L. Junkins. *Optimal Estimation of Dynamic Systems*. Chapman & Hall/CRC, Boca Raton, FL, 2004.

[2] D. A. Danielson, B. Neta, and L. W. Early. Semianalytic satellite theory (SST): Mathematical algorithms. Technical report, Naval Postgraduate School, 1994.

[3] K. J. DeMars. *Nonlinear Orbit Uncertainty Prediction and Rectification for Space Situational Awareness*. PhD thesis, Faculty of the Graduate School of The University of Texas at Austin, 2010.

[4] K. Fujimoto and D. J. Scheeres. Non-linear propagation of uncertainty with non-conservative effects. 2012. Presented at the *AAS/AIAA Spaceflight Mechanics Meeting*, Charleston, SC. AAS 12-263.

[5] K. Fujimoto, D. J. Scheeres, and K. T. Alfriend. Analytical nonlinear propagation of uncertainty in the two-body problem. *Journal of Guidance, Control, and Dynamics*, 35(2):497 – 509, 2012.

[6] D. Giza, P. Singla, and M. Jah. An approach for nonlinear uncertainty propagation: Application to orbital mechanics. 2009. Presented at the *2009 AIAA Guidance, Navigation, and Control Conference*, Chicago, IL. AIAA 2009-6082.

[7] J. Horwood, N. D. Aragon, and A. B. Poore. Gaussian sum filters for space surveillance: Theory and simulations. *Journal of Guidance, Control, and Dynamics*, 34(6):1839 – 1851, 2011.

[8] B. Jia, M. Xin, and Y. Cheng. Salient point quadrature nonlinear filtering. In *Proceedings of the 2011 American Control Conference*, 2011.

[9] D. King-Hele. *Theory of Satellite Orbits in an Atmosphere*. Butterworths, London, Great Britain, 1964.

[10] P. S. Maybeck. *Stochastic Models, Estimation and Control*, volume 2. Academic Press, New York, NY, 1982. pp. 159-271.

[11] J. W. McMahon and D. J. Scheeres. New solar radiation pressure force model for navigation. *Journal of Guidance, Control, and Dynamics*, 33(5):1418 – 1428, 2010.

[12] R. S. Park and D. J. Scheeres. Nonlinear mapping of gaussian statistics: Theory and applications to spacecraft trajectory design. *Journal of Guidance, Control and Dynamics*, 29(6):1367–1375, 2006.

[13] J. M. Picone, A. E. Hedin, D. P. Drob, and A. C. Aikin. NRLMSISE-00 empirical model of the atmosphere: Statistical comparisons and scientific issues. *Journal of Geophysical Research*, 107(A12):1468, 2002.

[14] D. J. Scheeres, D. Han, and Y. Hou. Influence of unstable manifolds on orbit uncertainty. *Journal of Guidance, Control, and Dynamics*, 24:573–585, 2001.

[15] D. J. Scheeres, F.-Y. Hsiao, R. Park, B. Villac, and J. M. Maruskin. Fundamental limits on spacecraft orbit uncertainty and distribution propagation. *Journal of Astronautical Sciences*, 54(3-4):505–523, 2006.

[16] M. Šimandl, J. Královec, and T. Söderström. Advanced point-mass method for nonlinear state estimation. *Automatica*, 42:1133 – 1145, 2006.

[17] D. Vallado. *Fundamentals of Astrodyamics and Applications*. Microcosm Press, Hawthorne, CA, third edition, 2007.